Crack formation and damage evolution during consolidation in TBM driven tunnel linings in fine-grained soils

Vincenzo De Gori1, Salvatore Miliziano2 and Armando de Lillis3
1 Sapienza, University of Rome, via Eudossiana 18, 00184, Italy. vincenzo.degori@gmail.com
2 Sapienza, University of Rome, via Eudossiana 18, 00184, Italy. salvatore.miliziano@uniroma1.it
3 Sapienza, University of Rome, via Eudossiana 18, 00184, Italy. armando.delillis@uniroma1.it

ABSTRACT

The paper deals with the numerical modelling of crack formation in segmental tunnel linings. A series of numerical analyses was conducted using the finite difference code FLAC2D. The primary aims of the analyses were to back-analyse the damage pattern observed in a TBM driven hydraulic tunnel excavated in clayey soils and to evaluate the safety level of the excavation assessing the stress and strain state of the lining.

The excavation of the tunnel and the lining installation were simulated in plane-strain undrained conditions, adopting the stress reduction method. To take into consideration the peculiar interaction mechanism, identified as the cause the damages, the stress release was differentiated based on the orientation along the tunnel wall. Two distinct modelling strategies were used to model the tunnel lining: at first, simple beam elements were used, then, small continuum elements and cable elements were employed to represent the concrete and the steel bars respectively. The implemented algorithm allowed to simulate explicitly the formation of the cracks and their progressive development. Finally, consolidation analyses were carried out to assess the evolution of the damage and the long-term stress and strain level of the lining.

The numerical analyses allowed to reproduce the observed damage pattern and to reliably evaluate the stress and strain state in the damaged lining. Furthermore, the long-term analyses showed that the consolidation process has a beneficial effect as the equalization of the pore pressures causes a reduction of the load eccentricity on the lining, thus progressively increasing the level of safety over time.
The investigation of the causes of the reported damage and its numerical modelling allowed to remark the importance of proper tail void grouting when excavating under high cover depths in squeezing soils.

Key Words: TBM, Cracks, Segmental Lining, Numerical Modelling, Cable, Tail Void Grouting.

1. INTRODUCTION

The cracking of precast reinforced concrete segments of TBM driven tunnel linings is a rather common issue. In most cases, it is caused by irregular jacks' forces or by improper assembly of the lining ring. These specific issues have been investigated by few authors. Chen & Mo (2009) and Cavalaro et al. (2011) studied the formation of local cracks concentrated around the circumferential seams, the hand holes and bolt holes. The loading tests performed by Molins & Arnau (2011) highlighted the development of cracks due to the hydraulic jacks' thrust, which was then numerically analysed by the authors through bi- and tri-dimensional models (Arnau & Molins, 2011). Litsas et al. (2015) investigated the influence of cracking on the stiffness and the capacity of segmental tunnel lining.

This paper investigates the numerical modelling of the formation on cracks in segmental tunnel linings with reference to a case study where the damage was imputable to a peculiar asymmetrical soil-lining interaction mechanism. In the first part, the observed damage pattern is described and the causes are identified. Then, the numerical model is illustrated and used to back-analyse the damage and to evaluate the stress and strain level in the lining. Finally, long-term analyses are carried out to investigate the effect of consolidation processes on the stress state of the damaged lining and on the safety of the excavation, forecasting two scenarios in which reparation works are carried out or not.

2. DESCRIPTION OF THE CASE STUDY: DAMAGE PATTERN AND CAUSES

The investigated tunnel is a small diameter hydraulic tunnel, recently excavated in southern Italy. The tunnel runs almost entirely through very homogeneous stiff clays, characterized by high consistency and medium plasticity; its length is about 4 km, under cover depths ranging from 10 m to 135 m. The piezometric height ranges from 3 m to 75 m above the tunnel axis.

The tunnel was driven by a small TBM operating in open mode. The machine's design and the construction procedures were aimed at minimizing the blockage risk and the stresses on the lining. Thus, the cutterhead overcut and the conicity of the shield were significant, to facilitate the steering of the TBM and increase the amount of stress relaxation around the tunnel. Moreover, the tail void grouting was not automated, instead the injection was designed to be performed manually, through the erector pin holes, at a distance of three lining rings from the tail of the shield. This design choice also was aimed at maximizing the stress release in the surrounding soil, while still maintaining the benefice of the grout injection stabilizing effect.

Under low cover depths, the construction proceeded normally and no problems were detected. As the cover depth increased towards its maximum value, a stretch of about 40 meters of the tunnel, near the excavation face, developed significant damage: sub-horizontal cracks were found at the intrados of the lining, roughly at the sides of the tunnel wall (see Figure 1), while at the crown some portion of concrete were detached, as showed in Figure 2. The workers reported hearing noises and noticing appreciable displacements of the lining segments in the damaged area. Through the erector pin holes, it was found a centimetric residual gap between the crown of the tunnel and the surrounding soil; at the springline and below, the soil was adherent to the lining.

Figure 1. Sub-horizontal cracks at the sides of the tunnel. Misaligned segments.

Figure 2. Concrete detachments in the upper part of the lining ring.

The depicted damage pattern was associated to a strongly asymmetrical closure of the surrounding soil onto the lining. In ordinary excavation condition, the ground closure onto the lining is practically symmetrical; in fact, even though the convergences are slightly different along the tunnel wall (the only exception being an isotropic geostatic stress state of the surrounding soil), the automated tail void grouting “fixes” the position of the surrounding soil before it experiences significant deformations. This ensures a globally compressive state of the lining and low variability of the normal forces along the wall.

The reported damaged was induced by the combined effect of two causes: a) the anisotropy of the geostatic stress state (K0 = 0.6), which, in cases of large deformations as the ones allowed by design in the problem at hand, induces a strongly plastic behaviour near the springlines and, consequently, higher convergences on the horizontal diameter than on the vertical one; b) the downward movement of the lining, which was not co-axial to the excavation profile because of i) the lack of proper application of the hydraulic jacks’ thrust on the lining segments during every phase of the construction and ii) the absence, or at least the significant delay, of the tail void grouting.

These improper construction procedures were not detected earlier because under low cover depths the convergences were very little, as the internal forces on the lining. In that situation, a delay in the tail void grouting doesn’t have a significant influence on the interaction mechanism. In Figure 3 are reported the so-called ground reaction curves, obtained assuming an isotropic geostatic stress state equal to the mean pressure. The curves show that, when excavating under high cover depths, the convergences in undrained condition were relevant. In such a case, delaying the grout injection of the tail void allows the surrounding soil to undergo significant deformations. This, in conjunction with the improper application the jacks’ thrust induced an asymmetrical interaction mechanism, as detailed in the following.

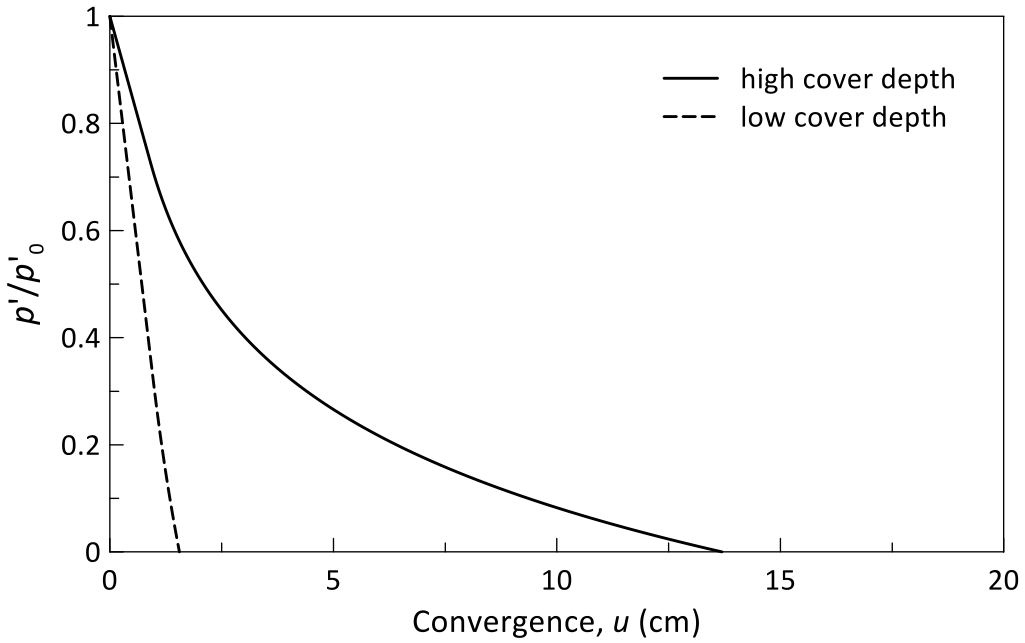

Figure 3. Undrained ground reaction curves.

Shortly after the causes of the damage were identified, the correct excavation procedures were restored, and the construction proceeded as designed. This was confirmed also by the monitoring data recorded in a successive section of the tunnel.

In Figure 4 is schematically reported the difference between the typical quasi-symmetrical interaction mechanism experienced in properly driven tunnels and the asymmetrical configuration identified as the cause of the damages.

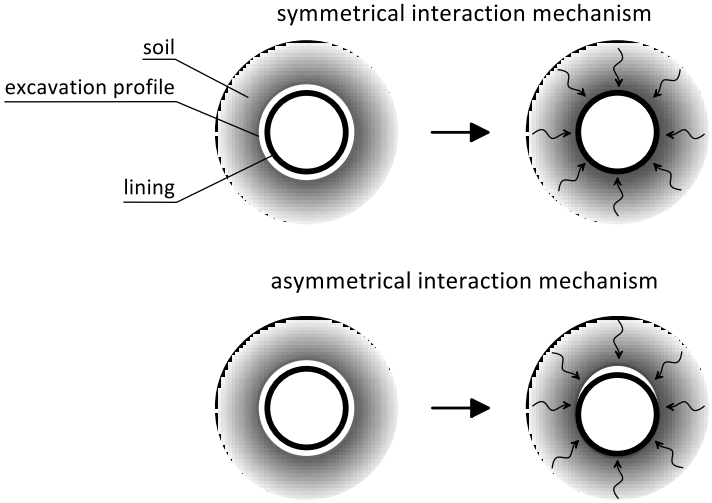

Figure 4. Interaction mechanisms.

The subsequent soil-lining interaction process is governed by the resulting pincer-like configuration. In its lower part, the lining is subject to an upward force applied by the soil heaving at the bottom of the tunnel, which is counteracted by the weight of the TBM and the backup trailer; on the sides, it is subject to a lateral, sub-horizontal, push exerted by the soil along the contact surface; in the upper part, a gap remains between the tunnel crown and the soil.

This peculiar interaction process is significantly different from the design assumptions and compatible with the damage pattern recorded in the tunnel. In fact, the strong compressive lateral push, in absence of proper confinement at the crown, causes the lining to ovalize increasing the vertical diameter, as schematically shown in Figure 5. The deformed lining suffers high bending moments tending the intrados fibres near the sides, which induce the horizontal cracks, while the concentration of stresses near the segments joints at the crown causes the concrete detachments.

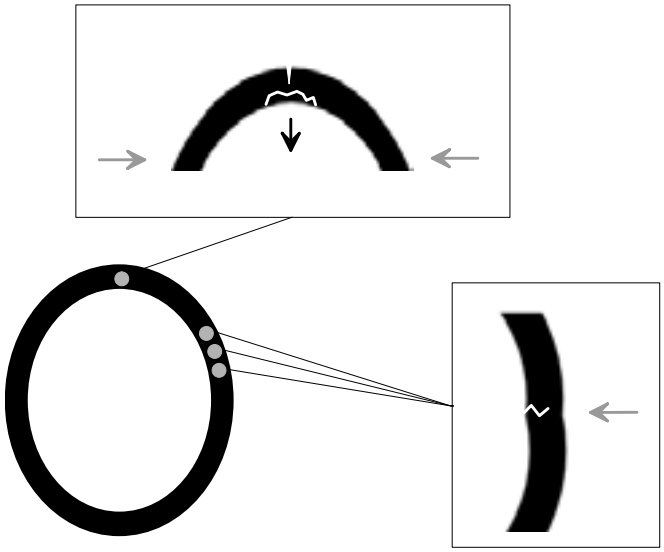

Figure 5. Deformed and damaged lining.

3. NUMERICAL ANALYSES

The interaction problem was studied through numerical analyses carried out using the finite difference computer code FLAC2D. The main objectives of the analyses were to confirm via back-analyses the causes of the damage and then to evaluate the stress and strain state of the lining and the safety of the excavation. As detailed in the following, since typical geotechnical modelling is not suitable to simulate neither the formation of cracks nor the composite nature of the structural elements, an original modelling strategy was developed and compared to the use of standard beam elements.

The excavation was simulated in plane-strain conditions, adopting a modified version of the stress reduction method. This method, which is the numerical adaptation of the convergence-confinement method (Panet & Guenot, 1982), reduces the three-dimensional problem to a bi-dimensional one, simulating the stress relaxation induced by the excavation and the advancement of the front through the progressive reduction of a fictitious set of forces applied to the tunnel wall.
The method consists of the following phases: 1) initialization of the geostatic stress state; 2) removal of the ground elements inside the tunnel and application of a set of forces equivalent to the initial stress state to the nodes describing the excavation boundary; 3) progressive reduction of the nodal forces up to a certain stress release factor λ, which has to be evaluated otherwise; 4) activation of the lining and release of the residual nodal forces.

Since the excavation was carried out in very low permeability clayey soils, the above phases were simulated in undrained condition. Consolidation analyses were then conducted to investigate the effects of the consolidation process on the damaged lining, taking into account the eventuality of reparation works aimed at restoring the damaged sections.

The soil's mechanical behaviour was simulated adopting a simple linear elastic perfectly plastic model with a Mohr-Coulomb failure criterion. In the following tables the main mechanical parameters and the geostatic stress state of the analysed control section are reported.

Due to the limited effect in comparison to the severity of the stress state (below 1%), the gradient of geostatic stresses was considered zero, assuming a stress state equal to that of the depth of the tunnel axis.

Table 1. Main soil mechanical parameters.

E'	c_u	$\varphi'_{eq\ (undrained)}$	$c'_{eq\ (undrained)}$	φ'	c'
(MPa)	(kPa)	(°)	(kPa)	(°)	(kPa)
210	600	20	0	23	0

Table 2. Geostatic stress state.

σ_v	σ_h	u
(kPa)	(kPa)	(kPa)
2350	1756	650

The lining ring is composed by 6 precast reinforced concrete segments, 25 cm thick, and has an external diameter of 3.9 m. In the analyses it was modelled adopting two different strategies. In a first phase, to study the global effects of the interaction process, it was modelled using beam elements, having mechanical properties equivalent to those of the actual precast segments of the lining: the young modulus is equal to 37 GPa and the thickness is 25 cm.

In a second phase, to investigate the formation of cracks and the consequent redistribution of stresses, the lining was modelled explicitly accounting for its composite nature: very small continuum elements were used to represent the concrete and cable elements to represent the steel bars. The concrete continuum elements behaviour is elastic perfectly plastic in compression and elastic perfectly fragile in tension with a Mohr-Coulomb failure criterion. The uniaxial compressive strength is equal to 49.8 MPa, the tensile cut-off is set to 4.4 MPa (this will be discussed shortly). The young modulus is 37 GPa. The steel bars have an elastic perfectly plastic behaviour, both in compression and extension, with a yield stress of 450 MPa and an elastic modulus of 210 GPa.

The lining model is showed in Figure 6. A detail of the contact area between segments is also reported. The contact surfaces are endowed with a frictional behaviour, thus relative displacements are allowed. The entire calculation grid is 170x170m, large enough to minimize the boundary effects.

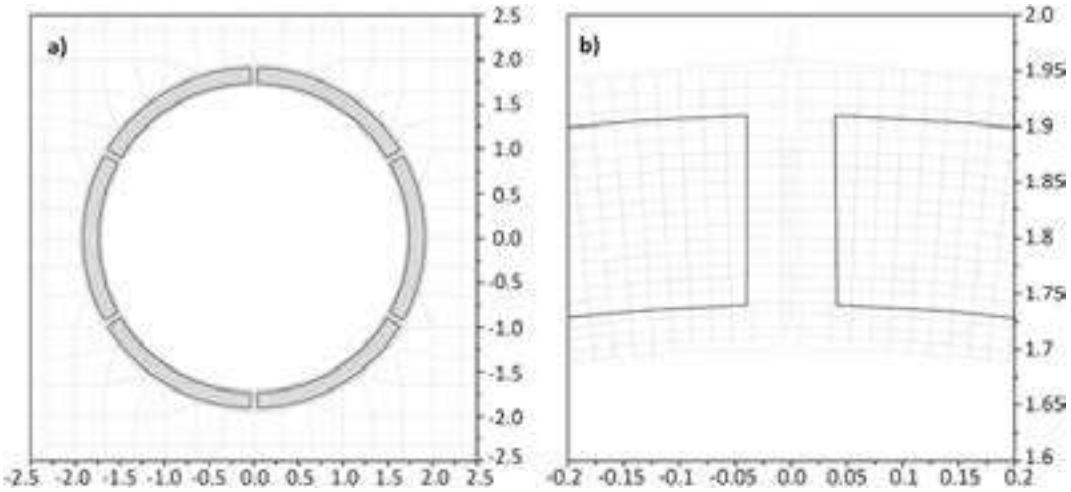

Figure 6. a) lining model with cable elements; b) detail of the segments contact area.

To simulate the stress development and the crack formation in the lining, an incremental procedure was adopted, sub-dividing the stress release in small perturbations of the equilibrium state. Moreover, the concrete tensile cut-off was updated step-by-step to avoid the development of plastic zones due to fluctuation of the unbalanced forces during numerical resolution. To this aim, at first the tensile cut-off was set to be very high, then, after every calculation step, the stress level was checked, and the resistance set to zero if the tensile cut-off was attained in the zone. In such cases, the zone's mechanical behaviour was turned into an extremely soft elastic one, virtually representing part of a crack in the lining. This procedure allowed to simulate the progressive cracking of the lining segments and the stress redistribution inside the structural element.

The following is divided in two parts: 1) short-term analyses, aimed at back-analysing the observed damage framework, confirm its causes and evaluate the lining's stress state; 2) consolidation analyses, conducted hypothesizing two scenarios in which reparation works have been carried out or not, aimed at predicting the system's long-term behaviour.

3.1. Back-analyses of the short-term behaviour

To reproduce the interaction process identified as the cause of the damage, the stress reduction method was adapted as follows: the stress reduction factor, which is usually assumed constant for a chosen section, was assumed to be variable along the excavation profile. A series of parametric analyses was conducted to define a distribution of λ able to reproduce the observed damage framework, following these guidelines: a) total stress release at the tunnel crown; b) partial stress release at the sides; c) low stress release in the invert area. The residual gap above the tunnel crown was assumed to be as large as a 60° circle arch symmetrical to the vertical axis. The parametric analyses led to the following stress release factors (prior to the installation of the lining): 100 % at the crown, 80% at the springline, 50% at the invert.

3.1.1. Beam analysis results

The forces arising in the lining in undrained condition are reported in Figure 7.

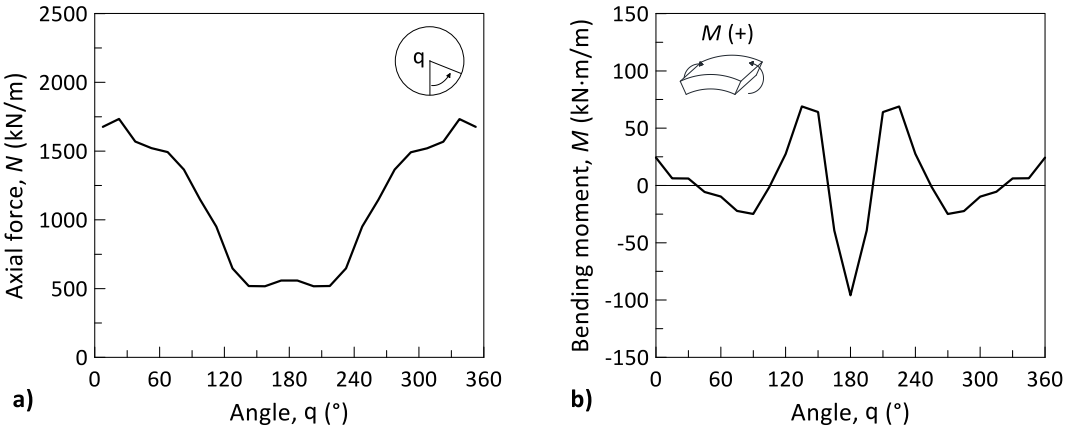

Figure 7. Internal forces in the lining: a) axial forces; b) bending moment.

The interaction process governed by the imposed stress reduction distribution induces minimum axial forces in the upper part of the lining. In the same area, significant and highly volatile bending moments develop. This corresponds to a high eccentricity of the stress state, particularly at the crown and in the area between 30° and 45° from the vertical axis.

It should be highlighted that this stress state is induced by the absence of proper confinement in the upper part of the lining, numerically simulated by the total stress relaxation. The deformed lining suffers a 3 cm increase of the vertical diameter. Figure 8 shows the distribution of the eccentricity along the lining:

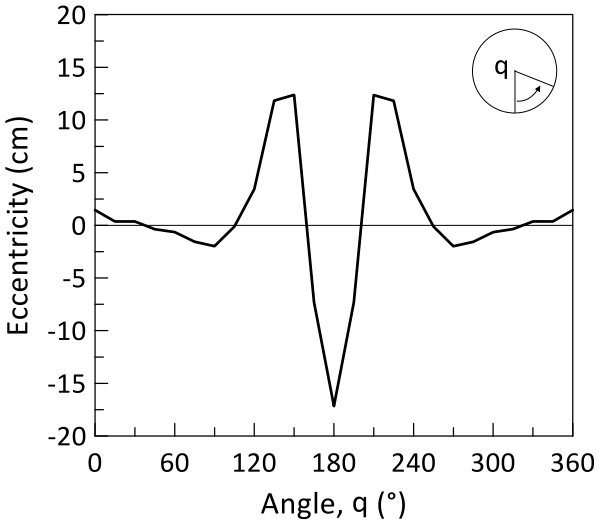

Figure 8. Load eccentricity on the lining.

The described stress state is associated with the development of significant tensile stresses in the upper part of the lining, definitely sufficient to cause structural damage. Nonetheless, this modelling strategy is not adequate to further investigate neither the formation of cracks nor the subsequent redistribution of the stress state, hence the development of the second lining model.

3.1.2. Cable analysis results

In Figure 9 the development of cracks in the numerical model is showed: a main and a secondary set of cracks can be seen. Their position is roughly the same of the maximum eccentricity tending the intrados fibres found in the beam analysis, and similar to the observed damage pattern. The main cracks resulting from the analysis have a width of 2.8 mm, comparable to those observed on site. At the extrados of the crown, no cracks are formed because of the presence of the joint.

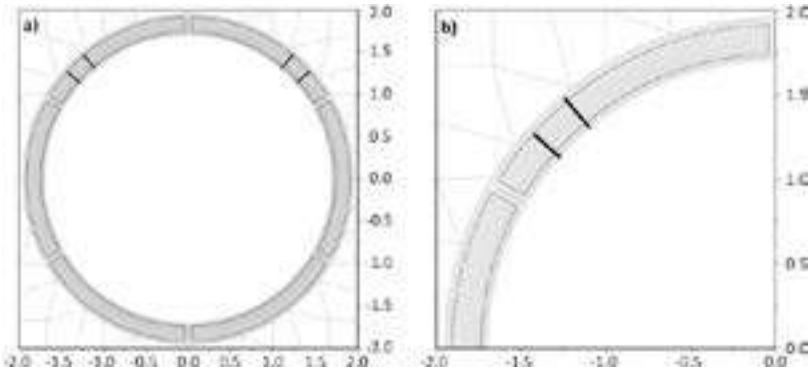

Figure 9. a) formation of cracks in the lining b) mesh detail.

The maximum and minimum principal stresses contours in the concrete are reported in Figure 10. After the formation of the cracks, the circumferential stress tends to zero where the tensile resistance is attained. The stress redistribution allows to reach the equilibrium through an increase of the axial force in steel bars (Figure 11a), contextual to the rise of the neutral axis in the cracked section. The strong compression of the intrados fibres at the crown is compatible with the observed detachment of concrete portions near the segments contact.

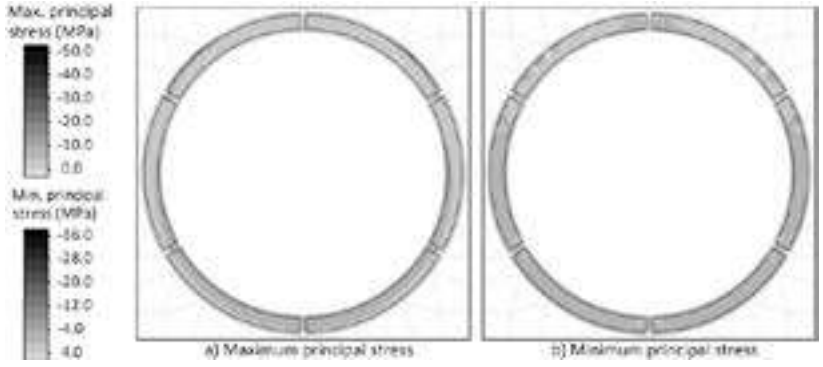

Figure 10. Principal stresses contours in the concrete.

In the damaged area, the cracking induces a higher work rate of the steel bars near the intrados, which are strongly elongated (1.9% maximum axial strain) and subject to a tensile stress equal to the yield stress, as shown in Figure 11. The steel bars at the extrados are subject to a tensile stress of about 190 MPa, thus are not yielded.

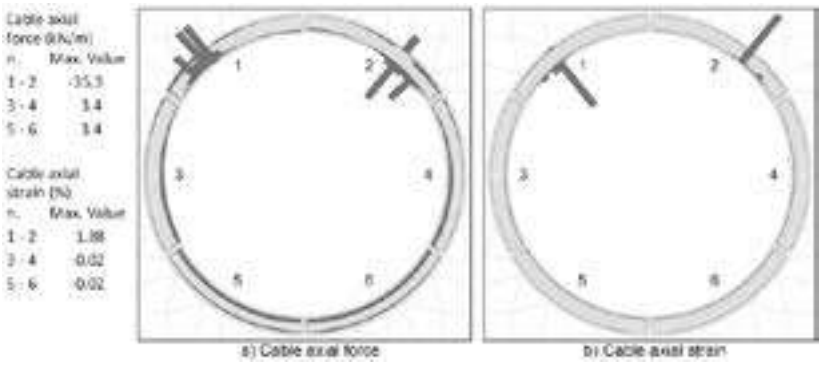

Figure 11. Axial forces and axial strains in the steel bars.

Even though the lining suffers a significantly plastic stress and strain state, the soil-lining system is globally stable due to the ductility reserves of the composite structural section.

3.2. Prediction of the long-term behaviour

The long-term behaviour was simulated conducting consolidation analyses, adopting both numerical models of the lining.

3.2.1. Beam analyses results

In the beam analyses, two scenarios were simulated: one in which the residual gap is still present at the crown and another in which the gap has been closed with an additional grout injection. The resulting internal forces in the lining are reported in Figure 12 and compared with the undrained results. The eccentricity of the stress state is reported in Figure 13.

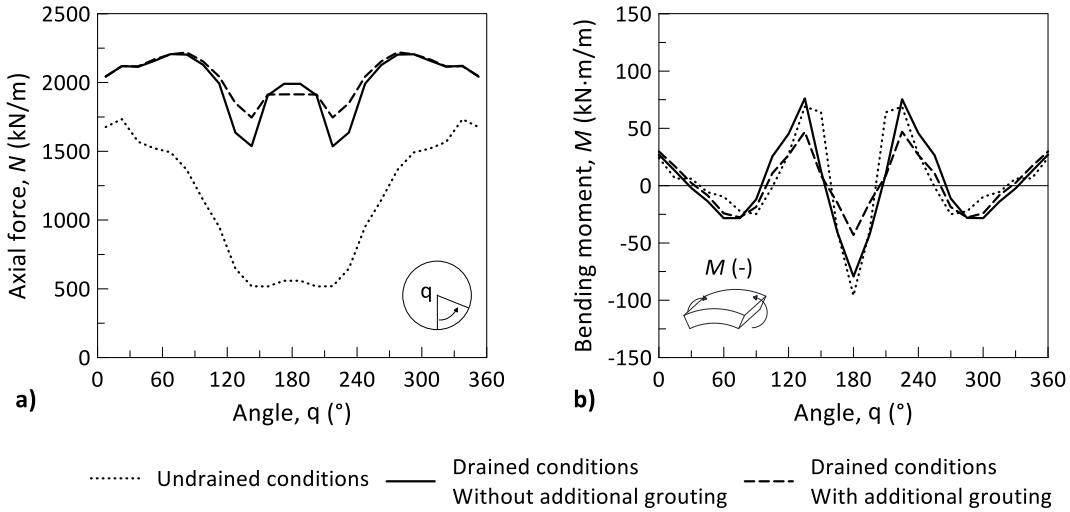

Figure 12. Internal forces with and without additional grout: a) axial forces; b) bending moments.

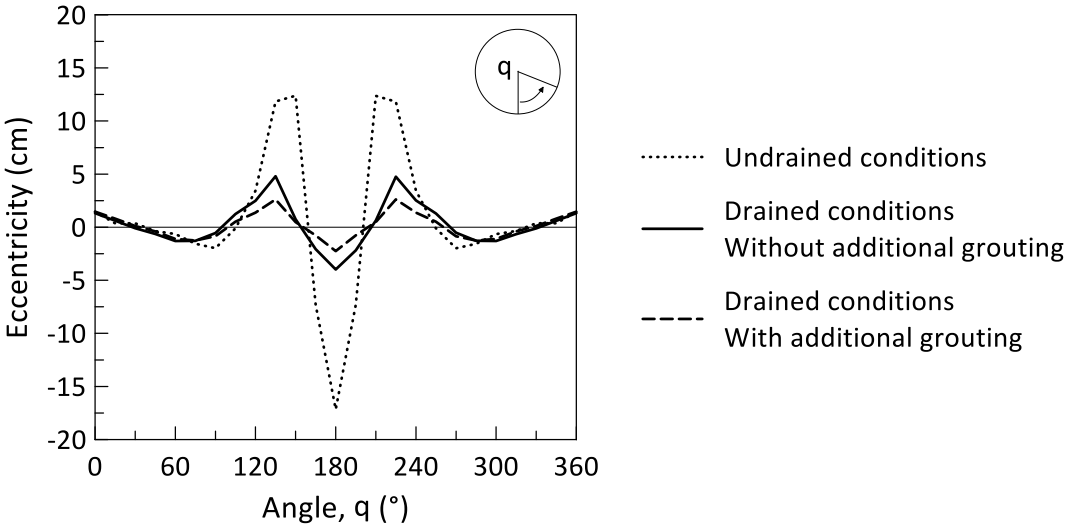

Figure 13. Load eccentricity on the lining with and without additional grouting.

In drained conditions, the eccentricity of the stress state decreases drastically and becomes lower than the limit one (about 5 cm) in both the simulated scenarios. The reduction is largely due to the increase in axial force associated with the consolidation process.

In the scenario without additional grouting, the evolution of the stress state during the consolidation induces additional displacements at the crown, which comes into contact with the lining, restoring a more ordinary configuration. This increases the compressive state of the lining and has a significant confinement effect. In the scenario with additional injection, the beneficial effect of the consolidation is even more apparent, as showed by the greater homogeneity of the axial forces and the lower bending moments near the crown.

3.2.2. Cable analyses results

In the cable analyses also, two scenarios were forecasted: one in which the concrete is cracked until the openings are closed by the compressive effect of the consolidation process; another in which the cracks have been repaired, thus the whole structural section is active. In both scenarios, the additional grout injection filling the residual gap above the crown was assumed.

In scenario 1, without reparation of the cracks, the results show that in drained condition the lining is entirely compressed (Figure 14).

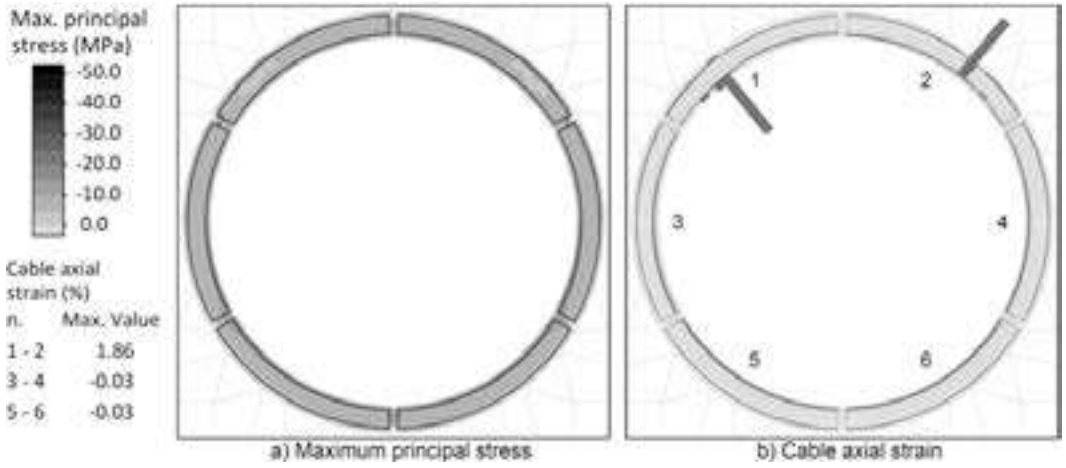

Figure 14. Maximum principal stress contours in the concrete and axial strains in the steel bars without reparation.

Due to the consolidation process, a progressive reduction of the tensile stress and a contextual shortening of the steel bars take place, inducing the closure of the cracks. Once the cracks are closed, the contribution of the concrete is re-activated and circumferential stresses develop at the intrados. In drained conditions the compressive stress in the concrete is 5÷10 MPa, while in the intrados steel bars is about 20 MPa with a residual elongation of about 1.5%.

The results obtained assuming the second scenario are reported in Figure 15. The reparation of the cracks impedes a significant shortening of the steel bars and the consequent turning of the tensile stresses into compressive ones. In detail, with respect to the undrained conditions, the shortening is limited to 0.02% and the tensile stress decreases of about 50 MPa. The concrete is subject to a compressive stress of about 10÷20 MPa, higher than that resulting from the first scenario.

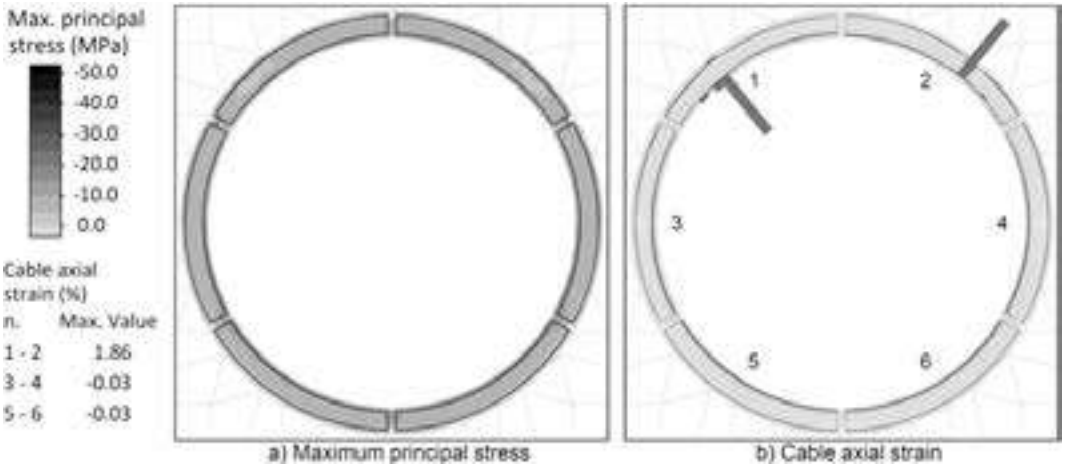

Figure 15. Maximum principal stress contours in the concrete and axial strains in the steel bars with reparation.

4. CONCLUSIONS

The paper presented the results of a set of 2D numerical analysis aimed at back-analysing the lining damage framework observed in a case study and at predicting the long-term behaviour of the damaged tunnel.

To simulate the asymmetrical interaction mechanism, the well-known stress reduction method was adapted. The analyses were performed implementing a distribution of stress release factors variable along the tunnel wall. Since usual geotechnical modelling is not adequate to reproduce the formation of cracks and the redistribution of stresses in damaged sections, an original modelling strategy was developed: the concrete was modelled using very small continuum elements while the steel bars were modelled using cable elements.

The analyses showed that the reported damage pattern was compatible with the peculiar interaction mechanism identified. Moreover, the analyses allowed to reliably evaluate the stress and strain state of the damaged lining, confirming that the structural element is stable in its damaged configuration.

Consolidation analyses were conducted to investigate the long-term behaviour of the damaged lining, assuming the eventuality of reparation works. The results showed that the consolidation process has a beneficial effect on the damaged lining, progressively increasing the safety of the excavation.

The study remarks the importance of proper tail void grouting when excavating under significant cover depths in squeezing soils. The grout injection, in fact, fixes the excavated profile before it can develop significant deformations, inducing a quasi-symmetrical interaction mechanism, which produces more homogeneous forces on the lining.

REFERENCES

Arnau, O., & Molins, C. (2011). Experimental and analytical study of the structural response of segmental tunnel linings based on an in situ loading test.
Part 2: Numerical simulation. Tunnelling and Underground Space Technology, 26(6), 778-788.
Cavalaro, S. H. P., Blom, C. B. M., Walraven, J. C., & Aguado, A. (2011). Structural analysis of contact deficiencies in segmented lining. Tunnelling and Underground Space Technology, 26(6), 734-749.

Chen, J. S., & Mo, H. H. (2009). Numerical study on crack problems in segments of shield tunnel using finite element method. Tunnelling and underground space technology, 24(1), 91-102.

ITASCA. 2005. FLAC2D, Fast Lagrangian Analyses of Continua, version 5.0, User's manual. Itasca Consulting group, Minneapolis.

Litsas, D., Pateriannaki, G., & Kavvadas, M. (2015). Investigation of the influence of cracking on the stiffness and capacity of segmental tunnel lining. In Promoting Tunnelling in See Region, WTC 2015.

Molins, C., & Arnau, O. (2011). Experimental and analytical study of the structural response of segmental tunnel linings based on an in situ loading test.: Part 1: Test configuration and execution. Tunnelling and Underground Space Technology, 26(6), 764-777.
Panet, M., & Guenot, A. (1982). Analysis of convergence behind the face of a tunnel. In Tunnelling 82. The Institution of Mining and Metallurgy, London.